TRANSVERSE AND LONGITUDINAL EDGE EFFECTS IN A RECTANGULAR MHD CHANNEL

N. G. Nemkova

Zhurnal Prikladnoi Mekhaniki i Tekhnicheskoi Fiziki, Vol. 10, No. 4, pp. 3–13, 1969

It is well known that in the case of magnetic field termination at the end of the electrode zone the current crossflow in the longitudinal section of the channel reduces the value of the power and leads to reduction of the generator efficiency [1, 2]. In order to exclude the end losses, it has been suggested [3, 4] that the magnetic field be extended beyond the electrode zone or that nonconducting barriers be located at the entrance to and exit from the electrode zone. If the magnetic field is extended beyond the electrode zone, the power increase exceeds the dissipation increase and the generator efficiency reaches its maximum value when the magnetic field is extended to infinity.

If we examine three-dimensional problems, the closed transverse currents increase significantly the value of the Joule dissipation even for very small boundary layers [5].

In the following we study the three-dimensional electric field distribution for stationary flow of an isotropically conducting fluid in a MHD channel with semi-infinite electrodes and calculate the Joule dissipation, power, and efficiency of the generator.

1. Consider a rectangular channel ($|x| < \infty$, $|y| < \delta$, $|z| < a$) whose walls are everywhere nonconducting (Fig. 1) except for the two semi-infinite electrodes $x > 0$, $y = \pm\delta$.

Through the channel flows an electroconductive fluid with constant conductivity σ and given velocity V(x, y, z). The channel is located in the external magnetic field $\mathbf{B} = \mathbf{B}(x, y, z)$, which is negligibly distorted by the induced currents.

Then, following [6], the current and potential distributions can be found from the equation

$$\Delta\varphi = \mathbf{B}\,\mathrm{rot}\,\mathbf{V} \tag{1.1}$$

with the following limiting conditions

$$\varphi = \pm\varphi_e \quad \text{for } y = \pm\delta, \quad x > 0 \tag{1.2}$$

$$\begin{gathered} j_y = \sigma\left(-\frac{\partial\varphi}{\partial y} + f_\pm\right) = 0 \quad \text{for } y = \pm\delta, \quad x < 0 \\ j_z = \sigma\left(-\frac{\partial\varphi}{\partial y} + g_\pm\right) = 0 \,\text{for } z = \pm a, \quad |x| < \infty \\ f_\pm(x, z) = \frac{\mathbf{V}\times\mathbf{B}}{c}\Big|_{y=\pm\delta}, \quad g_\pm(x, y) = \frac{\mathbf{V}\times\mathbf{B}}{c}\Big|_{z=\pm c} \\ \mathbf{B}\to 0, \quad \frac{\partial V}{\partial x}\to 0, \quad \varphi\to 0 \quad \text{for } x\to -\infty \\ \mathbf{B}\to\mathbf{B}_\infty(y, z), \quad \mathbf{V}\to V(y, z)e_x, \quad \frac{\partial\varphi}{\partial x}\to 0 \text{ for } x\to +\infty \end{gathered} \tag{1.3}$$

We assume that the velocity is a symmetric function with respect y and z and that $B_\infty(x, z)$ is a symmetric function with respect to z.

We introduce the auxiliary potential $\psi = \varphi - \varphi_0$, where $\varphi(x, y, z)$ is the unknown solution of the problem and $\varphi_0(x, y, z)$ is the solution of (1.1) with boundary conditions (1.3)–(1.4) for $|x| < \infty$, i.e., the solution of the analogous problem for the channel with everywhere nonconducting walls.

Then we obtain the Laplace equation for ψ

$$\Delta\Psi = 0 \tag{1.5}$$

and the boundary conditions

$$\psi = \pm\psi_e(x, \pm\delta, z) = (\mp\varphi_e) - \varphi_0(x, \pm\delta, z) \quad (y = \pm\delta,\ x > 0) \tag{1.6}$$

$$\partial\psi / \partial y = 0 \text{ for } y \pm \delta,\ x < 0; \quad \partial\psi / \partial z = 0 \text{ for } y = \pm\delta,\ |x| < \infty \tag{1.7}$$

$$\psi \to 0 \text{ for } x \to -\infty, \quad \partial\psi / \partial x \to 0 \quad \text{for } x \to +\infty \tag{1.8}$$

The problem solution for $\psi = \varphi - \varphi_0$ is sought in the form of the expansion

$$\psi = \frac{\psi_0}{2} + \sum_{k=1}^{\infty} \psi_k(x, y) \cos\frac{\pi k z}{a} \tag{1.9}$$

$$\psi_e = \frac{\psi_{e0}}{2} + \sum_{k=1}^{\infty} \psi_{ek}(x, \pm\delta) \cos\frac{\pi k z}{a} \tag{1.10}$$

The potential $\varphi_0(x, y, z)$ is [6]

$$\varphi_0 = \frac{1}{2} \sum_{k=1}^{\infty} \varphi_{n0} \sin r_n y$$

$$+ \sum_{k=1}^{\infty} \sum_{n=1}^{\infty} \varphi_{nk} \sin r_n y \cos\frac{\pi k z}{a}$$

$$r_n = \frac{\pi(n - 1/2)}{\delta} \tag{1.11}$$

Setting $y = \pm\delta$ and comparing coefficients in (1.10) and (1.11), we obtain

$$\psi_e = \pm\left(\frac{\psi_{e0}}{2} + \sum_{k=1}^{\infty} \psi_{ek} \cos\frac{\pi k z}{a}\right)$$

$$= \pm\left(\varphi_e - \frac{1}{2}\sum_{n=1}^{\infty} (-1)^{n+1}\varphi_{n0} - \sum_{k=1}^{\infty}\sum_{n=1}^{\infty} (1)^{n+1}\varphi_{nk} \cos\frac{\pi k z}{a}\right) \tag{1.12}$$

Hence

$$\psi_{e0} = -\varphi_e + \frac{1}{2}\sum_{n=1}^{\infty} (-1)^n \varphi_{n0}, \qquad \psi_{ek} = +\sum_{n=1}^{\infty} (-1)^n \varphi_{nk} \tag{1.13}$$

Thus, if the velocity profile and the magnetic field are given, the results of [6] define the coefficients of the expansion of the function $\varphi_0(x, y)$, while the coefficients of the expansion ψ_{e0}, ψ_{ek} are calculated from (1.13).

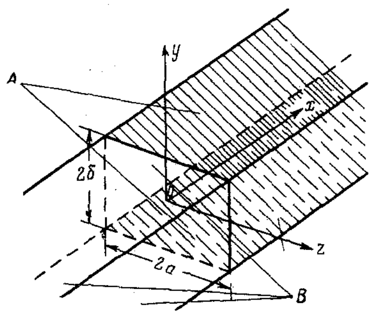

Fig. 1

We assume that the applied magnetic field is approximated by the step function

$$\mathbf{B} = \{0, 0, B_z(x)\}, \qquad B_z = 0 \ (x \leqslant -l), \quad B_z = B_0 \ (x > -l)$$

The velocity profile is specified so that it satisfies the no-slip conditions at the walls:

$$\mathbf{V} = \{V_x(y, z), 0, 0\}, \quad V_x(y, z) = V_0 \sum_{n=1}^{\infty} \chi_n(z) \cos r_n y$$

$$\chi_n(z) = \frac{V_n}{V_0}, \quad V_n = \int_{-\delta}^{\delta} V_x(y, z) \cos r_n y \, dy, \quad \chi_n(\pm a) = 0$$

Then

$$\varphi_{nk} = A\frac{r_n\chi_{nk}\delta}{\mu_{nk}^2}\frac{(\exp[-\mu_{nk}(x+e)]-1)}{2} = \frac{A}{2}a_{nk}(\exp[-\mu_{nk}(x+e)]-2)$$

$$A = \frac{V_0B_0}{\delta}, \quad \chi_{nk} = \frac{1}{2}\int_{-a}^{a}\chi_n(z)\cos\frac{\pi kz}{a}dz, \quad \mu_{nk}^2 = r_n^2+\lambda_k^2, \quad \lambda_k = \frac{\pi k}{a}$$

Substituting φ_{nk} into (1.13), we obtain

$$\psi_{e0} = \left[-\varphi_e + \frac{A}{4}\sum_{n=1}^{\infty}(-1)^n a_{n0}(\exp[-\mu_{nk}(x+l)]-2)\right]$$

$$\psi_{ek} = \frac{A}{2}\sum_{n=1}^{\infty}(-1)^n a_{nk}(\exp[-\mu_{nk}(x+\ )]-2) \tag{1.14}$$

The functions $\psi_k(x, y)$ must be found from the following system of equations, obtained after substituting ψ in the form (1.9) into the Laplace equation (1.5) and the conditions (1.6)–(1.8):

$$\Delta\psi_k - \lambda_k^2\psi_k = 0 \tag{1.15}$$

$$\psi_k = \pm\psi_{ek} \quad (y=\pm\delta,\ x>0), \qquad \frac{\partial\psi_k}{\partial x} = 0 \quad (y=\pm\delta,\ x<0) \tag{1.16}$$

$$\psi_k \to 0, \quad x\to-\infty, \qquad \partial\psi_k/\partial x\to 0, \quad x\to+\infty \tag{1.17}$$

2. Applying the two-sided Fourier transformation

$$\Phi_k(\alpha, y) = \frac{1}{(2\pi)^{1/2}}\int_{-\infty}^{\infty}\psi_k(x, y)\,e^{i\alpha x}\,dx$$

to (1.15), we obtain

$$\frac{d^2\Phi_k}{dy^2} - \gamma_k^2\Phi_k = 0, \qquad \gamma_k^2 = \lambda_k^2 + \alpha \tag{2.1}$$

Boundary condition (1.16) imposes on the function $\Phi_k(\alpha, y)$ the requirement that it be odd with respect to y. The solution of (2.1) satisfying this requirement takes the form

$$\Phi_k(\alpha, y) = A_k(\alpha)\,\mathrm{sh}\,\gamma_k y \tag{2.2}$$

If we introduce the functions

$$\Phi_k^+(\alpha, y) = \frac{1}{(2\pi)^{1/2}}\int_0^{\infty}\psi_k(x, y)\,e^{i\alpha x}\,dx$$

$$\Phi_k^-(\alpha, y) = \frac{1}{(2\pi)^{1/2}}\int_{-\infty}^{0}\psi_k(x, y)\,e^{i\alpha x}\,dx$$

$$(\Phi_k^+)' = \frac{1}{(2\pi)^{1/2}}\int_0^{\infty}\frac{\partial\psi_k}{\partial y}e^{i\alpha x}dx, \qquad (\Phi_k^-)' = \frac{1}{(2\pi)^{1/2}}\int_{-\infty}^{0}\frac{\partial\psi_k}{\partial y}e^{i\alpha x}dx$$

then, using (2.2), we obtain the system

$$\Phi_k^-(\alpha, y) + \Phi_k^+(\alpha, y) = A_k(\alpha)\,\mathrm{sh}\,\gamma_k y \tag{2.3}$$

$$\Phi_k^{-\prime}(\alpha, y) + \Phi_k^{+\prime}(\alpha, y) = A_k(\alpha)\gamma_k\,\mathrm{ch}\,\gamma_k y \tag{2.4}$$

We set $y = \pm\delta$ in these equations. Then $\Phi_k^+(\alpha, \delta)$ and $\Phi_k^{-\prime}(\alpha, \delta)$ are known by virtue of conditions (1.16). This makes it possible, after excluding the unknown function $A_k(\alpha)$, to obtain from (2.3) and (2.4) the equation in $\Phi_k^{+\prime}(\alpha, \delta)$ and $\Phi_k^-(\alpha, \delta)$:

$$\Phi_k^{+\prime}(\alpha, \delta) = \gamma_k\,\mathrm{cth}\,\gamma_k\delta[\Phi_k^-(\alpha, \delta) + \Phi_k^+(\alpha, \delta)] \tag{2.5}$$

This functional equation is the Wiener-Hopf equation. In order to study this equation the function $\Phi_k^{+\prime}(\alpha, \delta)$ is defined using (1.14):

$$\Phi_k^+(\alpha, \delta) = \frac{A}{(2\pi)^{1/2}}\left[\frac{\sigma_k}{i\alpha} + \sum_{n=1}^{\infty}(-1)^n a_{nk}\frac{\exp(-\mu_{nk}l)}{(\mu_{nk} - i\alpha)}\right]$$

$$\sigma_k = \begin{cases} -\dfrac{\varphi_e}{A} + \sum\limits_{n=1}^{\infty}(-1)^{n+1}a_{n0} & (k=0) \\ \sum\limits_{n=1}^{\infty}(-1)^n a_{nk} & (k \geqslant 1) \end{cases}$$

We factorize the function $K(\alpha) = \gamma_k\,\delta\,\mathrm{cth}\,\gamma_k\delta$:

$$K_k^{\pm}(\alpha) = \prod_{m=1}^{\infty}\frac{\sqrt{1 + b_m{}^2\lambda_k{}^2\delta^2} \mp b_m\delta i\alpha}{\sqrt{1 + a_m{}^2\lambda_k{}^2\delta^2} \mp a_m\delta i\alpha}, \quad a_m = \frac{1}{\pi m}, \quad b_m = \frac{1}{\pi(m - 1/2)}$$

Here $K_k^+(\alpha)$ and $K_k^-(\alpha)$ are functions of the complex parameter α, regular, respectively, in the half-planes

$$\alpha > -\tau_{1k} = -\frac{\sqrt{1 + a_1{}^2\delta^2\lambda_1{}^2}}{a_1\delta}, \quad \alpha < \tau_{1k}$$

After these transformations (2.5) takes the form

$$\begin{aligned} &\frac{\delta\Phi^+(\alpha, \delta)}{K_k^+(\alpha)} - \frac{A}{(2\pi)^{1/2}}\sum_{n=1}^{\infty}(-1)^n a_{nk}K_k^+(i\mu_{nk})\frac{e^{-\mu_{nk}l}}{(\alpha + i\mu_{nk})} \\ &+ \frac{A}{(2\pi)^{1/2}}K_k^+(0)\frac{\sigma_k i}{\alpha} = K_k^+(\alpha)\Phi_k^-(\alpha, \delta) \\ &+ \frac{A}{(2\pi)^{1/2}}\sum_{n=1}^{\infty}(-1)^n a_{nk}\frac{e^{-\mu_{nk}l}}{(\alpha + i\mu_{nk})}[K_k^+(\alpha) - K_k^+(i\mu_{nk})] \\ &- \frac{A}{(2\pi)^{1/2}}\frac{\sigma_k i}{\alpha}[K_k^-(\alpha) - K_k^-(0)] \end{aligned} \tag{2.6}$$

Let us study the region of regularity of this equation. We first examine the functions $\Phi_k^+(\alpha, \delta)$ and $\Phi_k^-(\alpha, \delta)$. By virtue of condition (1.17) the function $\psi_k \to 0$ as $x \to -\infty$; therefore we assume

$$|\psi_k| < C_1e^{-\beta_k x} \quad \text{for } x \to -\infty$$
$$(y = \text{const}, \ \beta_k = \text{const} \neq 0)$$

As an example, let

$$\beta_k = \mu_{1k} = \sqrt{\frac{\pi^2}{4\delta} + \frac{\pi^2K^2}{\alpha^2}}$$

Then, in accordance with [8], the function $\Phi_k^-(\alpha, y)$ will be regular for $\tau < \mu_{1k}$, where $\tau = \mathrm{Im}\,\alpha$. Since $d\psi_k/dx \to 0$ as $x \to \infty$, then $\Phi_k \to$ const for any fixed y as $x \to \infty$.

Consequently we have that $|\Phi_k| < C_2$ as $x \to +\infty$, i.e., the function $\Phi_k^+(\alpha, y)$ is regular for $\tau > 0$. Thus the region of regularity of the function $\Phi_k(\alpha, y)$ will be the strip $0 < \tau < \mu_{1k}$.*

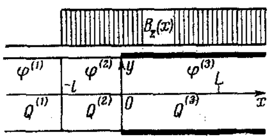

Fig. 2

We denote the right-hand and left-hand sides of (2.6) by $I_1(\alpha)$ and $I_2(\alpha)$, respectively. The functions appearing in $I_1(\alpha)$ are such that $I_1(\alpha)$ is regular for $\tau_k < \mu_{1k}$, while $I_2(\alpha)$ consists of functions which are regular for $\tau_k > 0$. Consequently, the region of regularity of the Wiener-Hopf equation is the strip $0 < \tau_k < \mu_k$. If we continue analytically the regular branches $I_1(\alpha)$ and $I_2(\alpha)$ into the entire plane, we obtain the function $I(\alpha) = I_1(\alpha) = I_2(\alpha)$, which is regular over the entire region.

*Inequalities (2.7) and (2.8) are obtained as a corollary of rather strong assumptions about the behavior of ψ_k as $x \to \pm\infty$. These assumptions are later confirmed by the constructed solution.

To estimate the growth of the functions $I_1(\alpha)$ and $I_2(\alpha)$ as $\alpha \to \infty$ and $\alpha \to -\infty$, we assume that the following conditions are met:

$$\frac{\partial\psi}{\partial y}(x, \delta) \to x^{1/2} \quad \text{for } x \to +0, \qquad \psi_k(x, \delta) \to \text{const} \quad \text{for } x \to -0$$

Then, following [8], we can state that the estimates

$$\Phi_k^{+\prime}(\alpha, \delta) \sim |\alpha|^{1/2}, \quad |\alpha| \to \infty; \qquad \Phi_k^-(\alpha, \delta) \sim |\alpha|^{-1}, \quad |\alpha| \to \infty$$

are valid, which together with the known estimates

$$K_k^+(\alpha) \sim |\alpha|^{1/2}, \quad |\alpha| \to \infty; \qquad K_k(\alpha) \sim |\alpha|^{1/2}, \quad |\alpha| \to \infty$$

makes it possible to clarify the behavior of the functions $I_1(\alpha)$ and $I_2(\alpha)$ as $|\alpha| \to \infty$ in the corresponding half-planes.

We find that

$$|I_1(\alpha)| < C_3|\alpha|^{-1/2} \text{ for } |\alpha| \to \infty, \ \tau < \mu_{1k}$$
$$|I_2(\alpha)| < C_4\alpha^{-1} \text{ for } \alpha \to \infty, \ \tau_k < 0$$

Then, on the basis of the generalized Liouville theorem, $I(\alpha) \equiv 0$ over the entire α-plane. Equating $I_1(\alpha)$ and $I_2(\alpha)$ to zero, we have two equations for determining the two unknown functions $\Phi_k^{+\prime}(\alpha, \delta)$ and $\Phi_k^-(\alpha, \delta)$. It suffices to know one of these functions in order to find $A(\alpha)$ from (2.3) and (2.4) and then obtain

$$\Phi_k(\alpha, y) = A_k(\alpha)\operatorname{sh}\gamma_k y = \frac{A}{(2\pi)^{1/2}}\Theta\Big[-\frac{i\sigma_k}{\alpha}$$
$$+\sum_{n=1}^{\infty}(-1)^n\frac{a_{nk}\exp(-\mu_{nk}l)}{\alpha+i\mu_{nk}}iK_k(i\mu_{nk})\Big], \qquad \Theta(\alpha, y) = \frac{K_k^+(\alpha)\operatorname{sh}\gamma_k y}{2\gamma_k\delta\operatorname{ch}\gamma_k\delta}$$

Application of the inverse Fourier transformation to Φ_k yields

$$\psi_k(x, y) = \frac{1}{(2\pi)^{1/2}}\int_{ic_k-\infty}^{ic_k+\infty}\Phi_k(\alpha, y)e^{-i\alpha x}d\alpha \tag{2.7}$$

The integration path lies in the strip of regularity of the function $\Phi_k(\alpha, y)$, i.e., $0 < c_k < \mu_{1k}$. Substituting $\Phi_k(\alpha, y)$ into (2.7), we find

$$\psi_k(x, y) = -\frac{Ai}{2\pi}\sigma_k\int_{-ic_k-\infty}^{ic_k+\infty}\Theta e^{-i\alpha x}d\alpha$$
$$-\frac{Ai}{2\pi}\sum_{n=1}^{\infty}(-1)^n a_{kn}K_k(i\mu_{nk})e^{-\mu_{nk}l}\int_{-ic_k-\infty}^{ic_k+\infty}\frac{\Theta e^{-i\alpha x}d\alpha}{(\alpha+i\mu_{nk})} \tag{2.8}$$

The integrals in (2.8) are calculated with the aid of residue theory separately for $x < 0$ and for $x > 0$. Knowing the coefficients of the expansion $\psi_k(x, y)$, we can use (1.9) to find $\psi(x, y, z)$ in both regions. Since the function $\varphi_0(x, y, z)$ calculated using the formulas of [6] has different analytic representations in the regions $x > -1$ and $x < -1$, the unknown potential $\varphi = \psi + \varphi_0$ has different representations in the three regions (see Fig. 2):

$$\varphi^1(x, y, z) = A\Big\{\sum_{s=1}^{\infty}\frac{1}{2}[(-1)^s b_{0s} - a_{0s}\exp\mu_{0s}l]\exp\mu_{0s}x\sin r_s y$$
$$+\sum_{k=1}^{\infty}\sum_{s=1}^{\infty}[(-1)^s b_{ks} - a_{ks}\exp\mu_{ks}l]\exp\mu_{ks}l\sin r_s y\cos\lambda_k z\Big\}$$
$$x \in [-\infty, -l] \tag{2.9}$$

$$\varphi^2(x, y, z) = A\Big\{\sum_{s=1}^{\infty}\frac{1}{2}[(-1)^s b_{0s}\exp\mu_{0s} + a_{0s}(2 - \exp[\mu_{0s}(x+l)])]\sin s_s y$$

$$+\sum_{k=1}^{\infty}\sum_{s=1}^{\infty}[(-1)^s b_{ks}\exp\mu_{ks}x + a_{ks}(2-\exp[-\mu_{ks}(x+l)])]\sin r_s y\cos\lambda_k z\}$$

$$x \in [-l, 0] \tag{2.10}$$

$$\varphi^3(x, y, z) = A\Big\{h_0\frac{y}{\delta} + \sum_{s=1}^{\infty}\frac{1}{2}[(-1)^s c_{0s}\exp(-\nu_{0s}x)\sin p_s y$$

$$-2a_{0s}\sin r_s y] + \sum_{k=1}^{\infty}\Big[\frac{h_k}{\pi k d\,\mathrm{ch}\,\pi k a}\,\mathrm{sh}\left(\frac{\pi k y}{e}\right)$$

$$+\sum_{s=1}^{\infty}((-1)^s c_{ks}\exp(-\nu_{ks}x)\sin p_s y - 2a_{ks}\sin r_s y)\Big]\cos\lambda_k z$$

$$x \in [0, \infty] \tag{2.11}$$

In (2.9)–(2.11) we have introduced the notations

$$p_s = \frac{\pi s}{\delta}, \quad r_s = \frac{\pi(s-1/2)}{\delta}, \quad \lambda_k = \frac{\pi k}{a}, \quad a_{ks} = \frac{r_s\chi_{ks}\delta}{2\mu_{ks}^2} = \frac{a_{ks}^\circ}{\mu_{ks}^2}$$

$$\nu_{ks}^2 = p_s^2 + \lambda_k^2, \quad \mu_{ks}^2 = r_s^2 + \lambda_k^2$$

$$b_{ks} = \Big[\sigma_k + \sum_{n=1}^{\infty}(-1)^n a_{kn}^\circ\exp(-\mu_{kn}l)\frac{\mu_{ks}}{\mu_{kn}+\mu_{ks}}R(i\mu_{kn})\Big]R(i\mu_{ks})$$

$$c_{ks} = \Big[K_k(0)\sigma_k + \sum_{n=1}^{\infty}(-1)^n a_{kn}^\circ\exp(-\mu_{kn}l)\frac{\nu_{ks}}{\mu_{kn}-\nu_{ks}}R(i\mu_{kn})\Big]S(-i\nu_{ks})$$

$$R(\alpha) = \frac{K_k^+(\alpha)}{(\alpha\delta)^2}, \quad S(\alpha_0) = \frac{i}{p_s\nu_{ks}}\lim_{\alpha\to\alpha_0}K_k^+(\alpha)(\alpha-\alpha_0)$$

3. The current density, Joule dissipation, and power in the channel are calculated from the formulas

$$j_x = -\sigma\frac{\partial\varphi}{\partial x}, \quad j_y = -\sigma\left(\frac{\partial\varphi}{\partial y}+\frac{vB}{c}\right), \quad j_z = -\sigma\frac{\partial\varphi}{\partial z} \tag{3.1}$$

$$Q = \int_{-\infty}^{\infty}\int_{-a}^{a}\int_{-\delta}^{\delta}\frac{j^2}{\sigma}\,dx\,dy\,dz = Q^1 + Q^2 + Q^3 \tag{3.2}$$

$$N = 2\varphi_e I(\delta) \tag{3.3}$$

where $I(\delta)$ is the total current flowing through the electrodes into the external load.

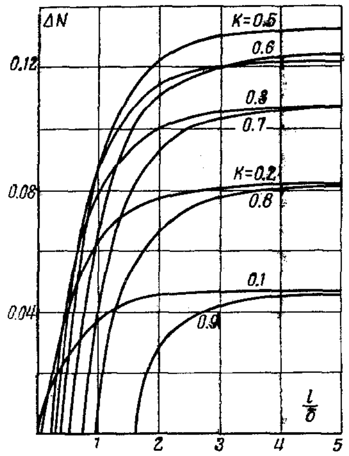

Fig. 3

The magnitudes of the currents and dissipation were calculated separately in each of three zones: in the pre-electrode zone without the magnetic field $[-\infty, -l)$, in the pre-electrode zone in the presence of the magnetic field $[-l, 0]$, and in the electrode zone in the presence of the magnetic field $[0, \infty]$. The Joule dissipation is denoted in these zones by the symbols Q^1, Q^2, Q^3, respectively. In zone 1 (Fig. 2) dissipation is caused only by current crossflow from zone 2 and is defined by the formula

$$Q^1 = \sigma a\delta A^2\Big[\sum_{s=1}^{\infty}\frac{1}{4}(\mu_{0s}(b_{0s}^2\exp(-2\mu_{0s}l) - 2a_{0s}b_{0s}\exp(-\mu_{0s}l) + a_{0s}^2)$$

$$+\sum_{k=1}^{\infty}\sum_{s=1}^{\infty}\mu_{ks}^2(b_{ks}^2\exp(-2\mu_{ks}l) - 2a_{ks}b_{ks}\exp(-\mu_{ks}l) + a_{ks}^2)\Big]$$

In zone 2 dissipation is caused by the longitudinal currents (the two-dimensional crossflow pattern of these currents is presented in [1]), and also by the closed transverse currents, which are analogous to the currents in the Hartmann problem. **For Q^2 we have the formula**

$$Q^2 = \sigma a\delta A^2\Big\{\sum_{s=1}^{\infty}[\xi_{0s}(\exp(-2\mu_{0s}l) - 1)\eta_{0s}(\exp(-\mu_{0s}l) - 1) + \zeta_{0s}l]$$

$$+\sum_{k=1}^{\infty}\sum_{s=1}^{\infty}[\xi_{ks}(\exp(-2\mu_{ks}l) - 1) + \eta_{ks}(\exp(-\mu_{ks}l) - 1) + \zeta_{ks}l]\Big\}$$

Here

$$\xi_{0s} = (\Omega_k^2\ a_{ks}^2 - b_{ks}^2)\mu_{ks}$$

$$\eta_{ks} = 2\Big[\Omega_k^2 a_{ks} - 4\Omega_k a_k b_{ks} + (-1)^{s+1}\frac{m_{ks}}{\mu_{ks}}(\Omega_k a_{ks} + b_{ks})\Big]$$

$$\zeta_{ks} = p_s^2 m_{ks}^2 + 4\mu_{ks}^2\Omega_k^2\ a_{ks}^2 + 4(-1)^{s+1}\ \Omega_k a_{ks} m_{ks}$$

The expression for a_{ks}, b_{ks}, μ_{ks}, r_s are written out above, and m_{kf}, Ω_k equal, respectively,

$$m_{ks} = \frac{r_s}{a\delta}\int_{-a}^{a} V_s B_z \cos\frac{\pi sz}{a}\,dz, \qquad \Omega = \begin{cases} 1/2 & k = 0 \\ 1 & k \geqslant 1 \end{cases}$$

From (3.5) follows

$$Q^2 \to 0 \quad \text{as} \quad l \to 0, \qquad Q^2 \to \infty \quad \text{as} \quad l \to \infty$$

Finally, in zone 3 dissipation is also caused by the longitudinal and transverse currents, but here in contrast with zone 2 part of the transverse currents makes a contribution to the useful power. As a result of the transverse currents the dissipation Q^3 is infinitely large. Therefore Q^3 was calculated for the fixed section of the channel with electrodes of length L:

$$Q^3 = A^2 a\delta\sigma\Big\{\frac{h_0^2 L}{\delta} + \sum_{s=1}^{\infty} P_s\cos^2(1 - \exp(-2\nu_{0s}L))$$

$$+\sum_{k=1}^{\infty}\Big[\Big(\delta_k + \sum_{s=1}^{\infty}\frac{\lambda_k^2\chi_{ks}^2\delta^2}{\mu_{ks}^2}\Big)L + \sum_{s=1}^{\infty}\nu_{ks}c_{ks}^2(1 - \exp(-2\nu_{ks}L))\Big]$$

The notations in the expression for Q^3 are the same as in (2.12)–(2.14). To calculate the power we resort to computation of the total current $I(\delta)$ using the formula

$$I(\delta) = \int_{a}^{\infty}\int_{-a}^{a} j_y\,dx\,dz$$

in which the upper integration limit is replaced by L, thereby assuming that the electrodes have finite length. The potential at the electrodes can be expressed in terms of the load coefficient k:

$$\varphi_e = kV_{\langle u\rangle}B\delta$$

where $V_{\langle u\rangle}$ is the channel section-average velocity, and then formula (3.3) for the power is written as

$$N = 2\pi(V_{\langle u\rangle}B)^2\delta^2\sigma\frac{k}{d}\Big[\frac{(1-k)}{\pi}\frac{L}{\delta} + \frac{1}{2\delta^2}\sum_{s=1}^{\infty}\cos\Big(1 - \exp(-\nu_{0s}L)\Big)\Big]$$

4. The study of the values of the power, Joule dissipation, and efficiency of the generator is made under the assumption that edge effects show up only upon entry into the magnetic field and into the electrode zone and also that the electrodynamic parameters are practically unifromly distributed along the channel length. Then the power N and Joule dissipation Q can be considered as the sums of two terms: the first is the value of the power or dissipation which appears as a result of the edge effects owing to the displacement of the magnetic field beyond the electrode zone; the second term is the value of the power or dissipation which is directly proportional to the electrode length L (here the value of the power coincides with that calculated using one-dimensional theory). In the expressions for the power and

dissipation, assuming $L/\delta \gg 1$, we can neglect the exponentially decreasing (as $L \to \infty$) terms, i.e., terms reflecting the fact of current nonuniformities at the entrance to the electrode zone, such as the formation of closed loops in the longitudinal sections of the channel and curvature of the streamlines as they flow around these loops. Estimating the length L, for which we can neglect the terms containing L/δ in the exponent, we establish the limiting electrode length L beyond which we can consider the current and potential distributions constant along the channel, and the power and dissipation can be calculated using two-dimensional theory.

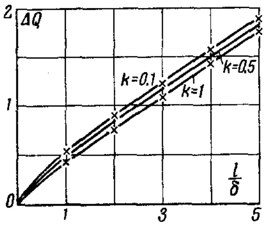

Fig. 4

To construct examples of the behavior of the generator power, Joule dissipation, and efficiency we specified a simple velocity profile

$$V = V_0\left(1 + \cos\frac{\pi z}{a}\right)\cos\frac{\pi y}{2\delta}$$

satisfying the no-slip condition at the channel walls and corresponding to boundary layers of considerable thickness (obviously the role of the transverse currents is overestimated in this case).

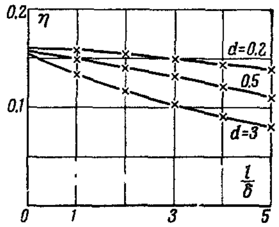

Fig. 5

In this case the power was calculated by means of the formula

$$N = 2\pi (V_{\langle U\rangle}B)^2\delta^3\sigma\frac{k}{d}\left[\frac{1-k}{\pi}\frac{L}{\delta} + \frac{(1-k)}{\pi^3}\sum_{p=1}^{\infty}\frac{P}{p(2p-1)}\right.$$
$$-\frac{1}{2\pi}\exp\frac{-\pi l}{2\delta}\sum_{p=1}^{\infty}\frac{P}{(2p-1)^2} - \frac{(1-k)}{\pi^2}\sum_{p=1}^{\infty}\frac{P}{p(2p-1)}\exp\frac{-\pi pL}{\delta}$$
$$\left.+\frac{1}{2\pi}\exp\frac{-\pi l}{2\delta}\sum_{p=1}^{\infty}\frac{P}{(2p-1)^2}\exp\frac{-\pi pL}{\delta}\right], \quad P = \prod_{m=1}^{\infty}\frac{m(m-p-1/2)}{(m-1)(m-p)} \tag{4.1}$$

The formula for calculating the Joule dissipation is not presented here because of the length of the expressions, but the Joule dissipation can be represented as a function of the parameters l/δ, L/δ, δ/a and the loading coefficient k in the form

$$Q = (V_{\langle u\rangle}B)^2\sigma\delta^3\frac{1}{d}\left\{\sum_{j=1}^{3}[a_j(k) + f_j(s_j, k)]\exp\frac{-\pi\nu_j l}{2\delta}\right.$$
$$+[b_j(d) + \Phi_j(s_j, d)]\exp\frac{-\pi\sqrt{d^2+0.25}\,\nu_j l}{\delta}$$
$$\left.+[C_j^1(k) + C_j^2(d)]\frac{L}{\delta} + \left[1 - \frac{1}{4(d^2+0.25)}\right]\frac{l}{\delta}\right\} \tag{4.2}$$
$$d = \frac{\delta}{a}, \quad s_j = \sum_{p=1}^{\infty} m_{pj}\exp\frac{-\pi p\mu_j L}{\delta}, \quad \nu_j = \begin{cases}0 & j=1\\ 1 & j=2\\ 2 & j=3\end{cases}, \quad \mu = \begin{cases}1 & j=3\\ 2 & j=1,2\end{cases}$$

The coefficients f_j, Φ_j ($j = 1, 2, 3$) will be functions of the infinite sums s_j, which contain in the general terms the infinite products m_{pj} and the parameter L/δ in the exponent. The terms in (4.2) which contain in the exponent only the parameter l/δ are due to the longitudinal currents flowing outside the electrode zone, i.e, the longitudinal edge effect;

those terms which contain in the exponent both l/δ and L/δ correspond to the longitudinal closed and nonuniform currents at the boundary of the electrode zone. The two terms which are linear in L/δ and l/δ are, respectively, the part of the dissipation owing to currents which are uniform across the section in the channel electrode zone and the part of the dissipation owing to the closed transverse currents, i.e., the transverse edge effect.

In (4.1) the last two terms can be neglected for $L/\delta \geq 4$, i.e., if the electrode length exceeds the channel height by a factor of two.

We denote the dimensionless parameters l/δ and L/δ by the letters g and h, respectively; then the expression for the power, reduced to the dimensionless form N^* by dividing by $(V_{\langle u\rangle}B)^2\sigma^3\sigma$, is written in the form

$$N^* = \frac{\Delta N(g, k)}{d} + \frac{N^\circ(h, k)}{d}$$

$$\Delta N(g, k) = \frac{2}{\pi} k(1-k) \sum_{p=1}^{\infty} \frac{P}{p(2p-1)} - k \exp - \frac{\pi}{2} g \sum_{p=1}^{\infty} \frac{P}{(2p-1)^2}$$

$$N^\circ(h, k) = 2k(1-k)h$$

The term $\Delta N(g,k)$ reflects only the influence of the edge effects. Calculations made on a BÉSM-3M computer showed that extending the magnetic field beyond the electrode zone increases the power. We see from the variation of ΔN with the magnetic field extension parameter g (Fig. 3) that ΔN reaches a maximum value for $k = 0.5$, just as $N^\circ(h,k)$ does. The ratio of the power increase ΔN owing only to the longitudinal edge effects to the power N^*, calculated inside the electrode zone, amounts to 6.5% for the magnetic field extension parameter $g = 3$, loading coefficient $k = 0.5$, and $h = 4$.

Dropping in (4.2) the sums analogous to those dropped in (4.1) for the power and reducing the expression for the Joule dissipation to dimensionless form, we write the expression thus obtained for Q^* as

$$Q^* = \Delta Q(g, k, d) + Q^\circ(h, k, d)$$

The quantity $\Delta Q(g,k,d)$ is the dissipation increment owing to the longitudinal and transverse currents outside the electrode zone. Neglect of the sums is valid for $h \geq 2$. A plot of ΔQ as a function of the field extension distance g for various loading coefficients k and fixed ratio $d = 3$ of the channel transverse dimensions is shown in Fig. 4. The calculations made for $d = 0.2$, 0.5, and 2 showed that, just as for the case $d = 3$ shown in Fig. 4, ΔQ increases linearly with respect to g as a result of the closed transverse currents, which also follows from (4.2).

The generator efficiency was calculated using the formula

$$\eta = \frac{N}{N+Q}$$

where the power N and dissipation Q were calculated using (4.1) and (4.2), in which h was taken equal to four. Figure 5 shows η as a function of the magnetic field extension for $k = 0.5$ and various d. It is obvious that the generator efficiency may decrease with extension of the magnetic field beyond the electrode zone since dissipation increases as a result of the transverse effect. If the power increment ΔN and, consequently, the entire value of N increases with extension of the magnetic field regardless of the channel geometry, then the generator efficiency is essentially determined by the parameter d — the ratio of the channel transverse dimensions.

The efficiency calculations showed that its value depends on the electrode zone length L, and for small L/δ the efficiency may reach its maximum value not with termination of the magnetic field at the end of the electrode zone but rather for some extension of the magnetic field beyond the electrode zone.

We note that as $d \to 0$, i.e., when the channel is stretched out in width and can be considered two-dimensional, the contribution of the transverse edge effect to the value of the dissipation diminishes.

In fact, in (4.2) the term reflecting the transverse edge effect has the form

$$Q^* = \left(1 - \frac{1}{4(d^2 + 0.25)}\right) \frac{l}{\delta} \qquad (Q^* \to 0,\ d \to 0)$$

If we examine Fig. 5 it is clear that for any finite d, no matter how small, beginning with some value of l/δ the curve begins to fall off as a result of the transverse edge effect. However, if at the same time $d \to 0$ and $l/\delta \to \infty$ the curve increases asymptotically, which confirms the result of two-dimensional theory stating that the efficiency reaches its maximum value when the magnetic field is extended to infinity. The low absolute values of the efficiency shown in Fig. 5 are explained by such factors as the velocity profile, which increases the transverse edge effects, the sharp termination of the magnetic field rather than a smooth dropoff of the field to zero outside the electrode zone, and the short generator length ($L/\delta = 4$). In actual installations account for these factors results in considerably higher efficiency.

The author wishes to thank S. A. Regirer for posing the problem and his interest in the study and V. I. Kovbasyuk for helpful discussions.

REFERENCES

1. A. B. Vatazhin, "Determining Joule dissipation in an MHD generator channel," PMTF, vol. 3, no. 5, 1962.

2. A. B. Vatazhin, "Some two-dimensional problems of current distribution in an electroconductive medium moving in a channel in a magnetic field," PMTF, vol. 4, no. 2, 1963.

3. G. W. Sutton, "Design considerations of a magnetohydrodynamic electrical power generator," Vista Astronaut., vol. 3, pp. 53–64, 1960.

4. A. B. Vatazhin and N. G. Nemkova, "Some two-dimensional problems of electric current distribution in an MHD generator channel with nonconducting barriers," PMTF, vol. 5, no. 2, 1964.

5. S. A. Regirer, "The influence of the boundary layer on the current distribution for conducting fluid flow in a channel," collection: Problems of Magnetohydrodynamics, vol. 3 [in Russian], Izd-vo AN LatvSSR, Riga, 1963.

6. S. A. Regirer, "Electric field in rectangular MHD channel with nonconducting walls," PMTF, vol. 4, no. 3, 1964.

7. A. B. Vatazhin and S. A Regirer, "Approximate calculation of current distribution for flow of a conducting fluid through a channel in a magnetic field," PMM, vol. 26, no. 3, 1962.

8. A. B. Vatazhin, "The solution of some edge problems of MHD," PMM, vol. 2, no. 5, 1961.

9. B. Noble, Methods Based on the Wiener-Hopf Technique [Russian translation], Izd-vo inostr. lit., Moscow, 1962.

6 January 1969

Moscow